First measurement of the Ti(e,e^{′})X cross section at Jefferson Lab

H. Dai *et al.* (Jefferson Lab Hall A Collaboration)

Phys. Rev. C **98**, 014617 — Published 25 July 2018

DOI: 10.1103/PhysRevC.98.014617

JLAB-PHY-18-2656
SLAC-PUB-17200

First Measurement of the Ti(e, e')X Cross Section at Jefferson Lab

H. Dai,[1] M. Murphy,[1] V. Pandey,[1,*] D. Abrams,[2] D. Nguyen,[2] B. Aljawrneh,[3] S. Alsalmi,[4] A. M. Ankowski,[1,5,†] J. Bane,[6] S. Barcus,[7] O. Benhar,[8] V. Bellini,[9] J. Bericic,[10] D. Biswas,[11] A. Camsonne,[10] J. Castellanos,[12] J.-P. Chen,[10] M. E. Christy,[11] K. Craycraft,[6] R. Cruz-Torres,[13] D. Day,[2] S.-C. Dusa,[10] E. Fuchey,[14] T. Gautam,[11] C. Giusti,[15] J. Gomez,[10] C. Gu,[2] T. Hague,[4] J.-O. Hansen,[10] F. Hauenstein,[16] D. W. Higinbotham,[10] C. Hyde,[16] C. M. Jen,[1] C. Keppel,[10] S. Li,[17] R. Lindgren,[18] H. Liu,[19] C. Mariani,[1] R. E. McClellan,[10] D. Meekins,[10] R. Michaels,[10] M. Mihovilovic,[20] M. Nycz,[4] L. Ou,[13] B. Pandey,[11] K. Park,[10] G. Perera,[18] A.J.R. Puckett,[14] S. Širca,[21,20] T. Su,[4] L. Tang,[11] Y. Tian,[22] N. Ton,[18] B. Wojtsekhowski,[10] S. Wood,[10] Z. Ye,[23] and J. Zhang[18]

(The Jefferson Lab Hall A Collaboration)

[1] *Center for Neutrino Physics, Virginia Tech, Blacksburg, Virginia 24061, USA*
[2] *Department of Physics, University of Virginia, Charlottesville, VA, 22904, USA*
[3] *North Carolina Agricultural and Technical State University, Greensboro, North Carolina, 27401, USA*
[4] *Kent State University, Kent, Ohio, 44242, USA*
[5] *SLAC National Accelerator Laboratory, Stanford University, Menlo Park, CA, 94025, USA*
[6] *The University of Tennessee, Knoxville, Tennessee 37996, USA*
[7] *The College of William and Mary, Williamsburg, Virginia, 23187, USA*
[8] *INFN and Dipartimento di Fisica, Sapienza Università di Roma, I-00185 Roma, Italy*
[9] *INFN, Sezione di Catania, Catania, 95123, Italy*
[10] *Thomas Jefferson National Accelerator Facility, Newport News, Virginia 23606, USA*
[11] *Hampton University, Hampton, Virginia, 23669, USA*
[12] *Florida International University, Miami, FL, 33181, USA*
[13] *Massachusetts Institute of Technology, Cambridge, Massachusetts, 02139, USA*
[14] *University of Connecticut, Storrs, Connecticut 06269, USA*
[15] *Dipartimento di Fisica, Università degli Studi di Pavia and INFN, Sezione di Pavia, I-27100 Pavia, Italy*
[16] *Old Dominion University, Norfolk, VA 23529, USA*
[17] *University of New Hampshire, Durham, New Hampshire, 03824, USA*
[18] *University of Virginia, Charlottesville, Virginia, 22908, USA*
[19] *Columbia University, New York, New York, 10027, USA*
[20] *Jozef Stefan Institute, Ljubljana 1000, Slovenia*
[21] *University of Ljubljana, Ljubljana, 1000, Slovenia*
[22] *Shandong University, Shandong, 250000, China*
[23] *Physics Division, Argonne National Laboratory, Argonne, Illinois 60439, USA*

To probe CP violation in the leptonic sector using GeV energy neutrino beams on current and future experiments using argon detectors, precise models of the complex underlying neutrino and antineutrino interactions are needed. The E12-14-012 experiment at Jefferson Lab Hall A was designed to perform a combined analysis of inclusive and exclusive electron scatterings on both argon ($N = 22$) and titanium ($Z = 22$) nuclei using GeV energy electron beams. The measurement on titanium nucleus provides essential information to understand the neutrino scattering on argon, large contribution to which comes from scattering off neutrons. Here we report the first experimental study of electron-titanium scattering as double differential cross section at beam energy $E = 2.222$ GeV and electron scattering angle $\theta = 15.541$ deg, measured over a broad range of energy transfer, spanning the kinematical regions in which quasielastic scattering and delta production are the dominant reaction mechanisms. The data provide valuable new information needed to develop accurate theoretical models of the electromagnetic and weak cross sections of these complex nuclei in the kinematic regime of interest to neutrino experiments.

The interpretation of the data collected by experimental studies of neutrino oscillations demands a fully quantitative description of neutrino interactions with the atomic nuclei comprising the detector [1]. Current and future neutrino experiments, such as the short- (SBN) [2] and the long-baseline (DUNE) [3] neutrino programs, will use detectors based on the liquid-argon time-projection chambers (LArTPCs) technology. In order to achieve the precision goals of these programs, the treatment of nuclear effects, which has been recognized as a major source of systematic uncertainty in ongoing experiments [4], has to be addressed. Realistic models of both neutrino- and antineutrino-argon interactions will be even more critical to future experiments, such as DUNE, aimed at pinning down charge-parity (CP) symmetry violation in the leptonic sector, because its determination with few percent precision requires accurate measurements of both neu-

* vishvas.pandey@vt.edu
† Present address: SLAC National Accelerator Laboratory, Stanford University, Menlo Park, CA, 94025, USA

trino and antineutrino oscillations. Failing to achieve this goal in a timely manner will deeply affect the sensitivity of DUNE to measure the CP violating phase (δ_{CP}), as discussed in [5].

Since the description of nuclear effects in a non isospin-symmetric nucleus, such as argon, must take into account the differences in the shell-model states occupied by protons and neutrons, and the information on neutrons cannot be directly extracted, one has to resort to studies of titanium nucleus. Owing to the fact that the neutron spectrum of $^{40}_{18}$Ar is mirrored by the proton spectrum of Ti, the Ti data will give access to the neutron spectral function of argon. Given the scarcity of electron-argon scattering experiments—the only available data on argon being the inclusive spectrum measured at Frascati National Laboratory using the electron-positron collider ADONE and a jet target [6]—we performed a dedicated experiment at Jefferson Lab (JLab), aimed at measuring inclusive and exclusive cross-sections on both argon and titanium targets, and extracting the proton [via Ar$(e,e'p)$] and neutron [via Ti$(e,e'p)$)] spectral functions of the argon nucleus in the kinematical region in which shell-model dynamics is dominant [7].

Electron-scattering experiments have provided a wealth of information on the nuclear response to electromagnetic interactions over a broad kinematic regime. Static form factors and charge distributions have been extracted from elastic scattering data, while measurements of inelastic cross sections have allowed for systematic studies of the dynamic response functions, which shed light on the role played by different reaction mechanisms. Finally, with the advent of continuous beam accelerators, a number of exclusive processes have been analyzed to unprecedented precision. The availability of the body of electron-nucleus scattering data has been essential to the development of theoretical models. Most notably, experimental studies of the $(e,e'p)$ process—in which the scattered electron and the knocked-out proton are detected in coincidence—have provided detailed information on proton spectral functions [8–11], the knowledge of which is needed to obtain the nuclear cross sections within the factorization scheme underlying the impulse approximation (IA). The description based on the IA and the spectral function formalism [12] has been successful in describing inclusive electron-scattering data in a variety of kinematic regimes [13–15], and has recently been be extended to the analysis of neutrino scattering [16–19]. However, due to the scarcity of available inclusive cross sections for argon and titanium, theoretical models of nuclear effects in electroweak interactions [20–26] cannot be currently validated in the kinematical region relevant for neutrino experiments.

The experiment E12-14-012 planned to perform a combined analysis of Ar and Ti inclusive and exclusive reactions collected high statistics data in JLab Hall A during February-March 2017. Here, we report the first results of the experiment, including the Ti$(e,e')X$ cross section at beam energy $E = 2.222$ GeV and electron scattering angle $\theta = 15.541$ deg and the corresponding electron-carbon cross section. Note that this is the first double differential Ti$(e,e')X$ cross section measured at the kinematics relevant for neutrino experiments, the previous studies on titanium target include [27–29]. The measurement of the C$(e,e')X$ cross section allowed a comparison with previous experiments, as well as a careful study of systematic uncertainties. In the (e,e') process $e + A \to e' + X$, an electron of four-momentum $k \equiv (E, \mathbf{k})$ scatters off a nuclear target A. The energy and emission angle of the scattered electron of four-momentum $k' \equiv (E', \mathbf{k}')$ are measured, while the hadronic final state is left undetected. The squared four-momentum transfer in the process is $q^2 = -Q^2$, with $q = k - k' \equiv (\omega, \mathbf{q})$.

The electron beam was provided by the Continuous Electron Beam Accelerator Facility (CEBAF) at JLab, with currents in excess of 10 μA. The beam current was monitored using two Beam Current Monitors (BCMs), which are resonant radio-frequency cavities. The position of the beam was monitored by two similar cavity types, Beam Position Monitors (BPMs). Beam size was measured with harp scanners, which also allowed the cavity monitor calibration. Beam position determination is important for vertex reconstruction and momentum calculation of the scattered electron. The beam was rastered, with a 2 mm $\times$ 2 mm raster system, in both vertical and horizontal directions, to reduce the beam current density and hence eliminate the possibility of melting the solid foil targets and minimize the local heating of the cryogenic hydrogen target. Both the carbon and titanium targets were foils of natural isotope composition, with a thickness of 0.167$\pm$0.001 g/cm^2 and 0.729$\pm$0.001 g/cm^2, respectively.

The scattered particles were momentum analyzed by two nearly identical spectrometers—the Left and a Right High-Resolution Spectrometers (HRSs)—equipped with detectors for tracking, timing and particle ID. The HRSs consist of 4 magnets (3 superconducting and 1 resistive) in a QQDQ configuration, where the Q indicates a quadrupole magnet and the D indicates a dipole magnet. This arrangement provided a large acceptance for both the angle and momentum, with a relative momentum resolution of $\sim 10^{-4}$, and pointing accuracy and angular resolution of $\sim 10^{-4}$ m and $\sim$10 mrad, respectively. The detector package, slightly updated with respect to the one in Ref. [30], consisting of vertical drift chambers (VDCs), threshold Čerenkov counters, scintillator detectors and a lead-glass calorimeters, provides data-acquisition triggering, tracking, and particle identification.

The scattered electrons were detected in the Left HRS positioned at $\theta = 15.541$ deg. The data acquisition was triggered, with an efficiency of 99.9%, when an electron fired the two scintillator detectors planes (with a logical AND) simultaneously with a signal in the gas Čerenkov detector. The electrons were identified by a gas threshold Čerenkov detector, mounted between two scintillator detector planes, with 99.9% efficiency and negligible pion contamination. The track trajectories were reconstructed

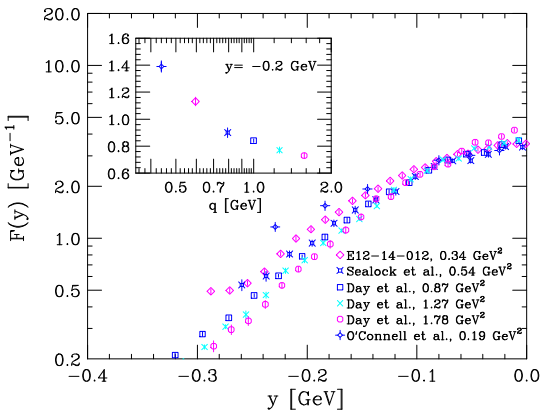

FIG. 1. (color online). Comparison between the scaling function $F(y)$ obtained from the E12-14-012 data on C, represented by diamonds, and those obtained from the data of O'Connell *et al.* [37], Sealock *et al.* [38], and Day *et al.* [39]. The inset shows the momentum transfer dependence of $F(y)$ at fixed $y = -0.2$ GeV. The data sets are labeled by the value of Q^2 corresponding to the top of the quasielastic peak.

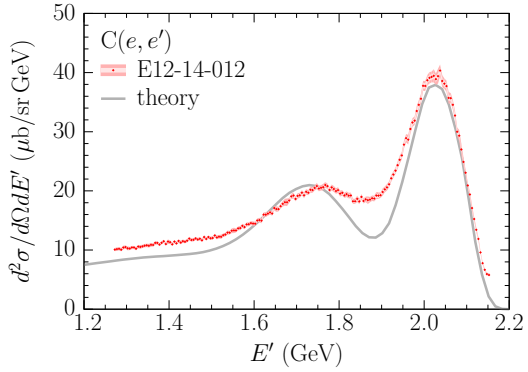

FIG. 2. (color online). Double differential cross section for the C(e,e') process measured at beam energy of 2.222 GeV and scattering angle of 15.541 deg. The inner and outer uncertainty bars correspond to statistical and total uncertainties, respectively. The solid line represents the theoretical results obtained within the formalism described in Refs. [12, 14, 15, 44].

in the detector stack using the VDCs with efficiencies of $\sim$ 95% for C and $\sim$ 92% for Ti, and then transported to the target utilizing a fitted reconstruction matrix obtained from a special optics calibration run. We required only one VDC track reconstructed in the final state for simplicity and purity purposes. The number of VDC reconstructed tracks in the case of the Ti target is slightly higher than for the C target, the difference in respective VDC efficiencies was as expected.

The cross section is extracted first computing the yield defined in both data and simulation as:

$$\text{Yield}^i = (N_S^i \times \text{DAQ}_{\text{pre-scale}})/(N_e \times LT \times \epsilon). \qquad (1)$$

Here, i is the ith bin in E', N_S^i represents the number of scattered electrons, N_e is the total number of electrons on the target, LT is the live-time, ϵ is the total efficiency and $\text{DAQ}_{\text{pre-scale}}$ is a factor that determines what fraction of the events gets recorded. The cross section in each bin i is computed as the product of the Monte Carlo (MC) cross section [31] times the ratio of the data to simulation yields. The MC cross section is a fit to existing data, including preliminary Hall C [32] data and includes radiative corrections computed using the peaking approximation [33] and Coulomb corrections implemented with an effective momentum approximation [34].

Over nearly five decades, a number of measurements of the electron-carbon cross section have been performed at different electron-scattering facilities around the world. A compilation of the available inclusive data can be found in Ref. [35]. In order to put our results in perspective, in Fig. 1 we compare the y-scaling function [36], $F(y)$, obtained from the cross section measured by the E12-14-012 experiment to those obtained from the data of Refs. [37–39], spanning a kinematical range corresponding to $0.20 \lesssim Q^2 \lesssim 1.8$ GeV^2. The occurrence of scaling in the variable, i.e. the observation that $F(y)$ becomes independent of the momentum transfer $|\mathbf{q}|$ in the limit of large $|\mathbf{q}|$, indicates that quasielastic scattering is the dominant reaction mechanism and final state interactions (FSI) between the knocked out nucleon and the residual nucleus are negligible. The scaling variable y, whose definition is given in Ref. [36], can be loosely identified with the component of the initial nucleon momentum parallel to the momentum transfer.

The main panel of Fig. 1 clearly shows that the data exhibit a remarkable scaling behavior at $y \approx 0$, corresponding to $\omega \approx Q^2/2M$, where M is the nucleon mass, while sizable scaling violations, to be mainly ascribed to FSI, are observed at large negative values of y. The momentum transfer dependence of $F(y)$ at $y = -0.2$ GeV, illustrated in the inset, demonstrates that in the kinematical setup of our experiment, corresponding to $|\mathbf{q}| \approx 600$ MeV, the effects of FSI are still significant. Overall, Fig. 1 shows that our results are fully consistent with those of previous experiments.

TABLE I. Contributions to the uncertainties associated with the measured C(e,e') cross sections. Numbers represents upper limit or range for the uncertainties that vary between kinematical regions.

1. Total statistical uncertainty	1.2%
2. Total systematic uncertainty	2.0–2.9%
a. Beam charge & Beam Energy	0.3%
b. Beam offset x&y	0.1%–0.4%
c. Target thickness	0.1%–0.4%
d. HRS offset x&y+ Optics	1.3%–2.0%
e. Acceptance cut(θ,ϕ,dp/p)	1.0%–1.4%
f. Calorimeter & Čerenkov cuts	0.01%–0.02%
g. Cross Section Model	0.1%–0.2%
h. Radiative +Coulomb Corr.	1.0–1.3%

Figure 2 shows the measured C(e,e') cross section as

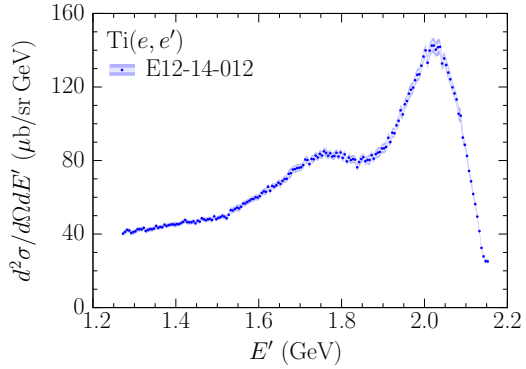

FIG. 3. (color online). Double differential cross section for the Ti(e,e') process measured at beam energy of 2.222 GeV and fixed scattering angle of 15.541 deg. The inner and outer uncertainty bars correspond to statistical and total uncertainties, respectively. The maximum uncertainties in the full kinematical range are provided.

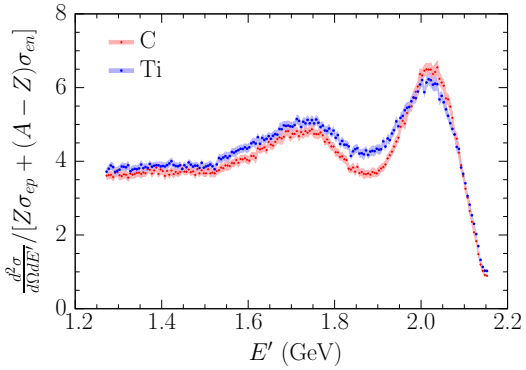

FIG. 4. (color online). Ratios defined by Eq.(3), computed using the measured carbon and titanium cross sections.

a function of the energy of the scattered electron, ranging from ∼1.2 GeV to ∼2.2 GeV with error bars up to ∼2.5%, corresponding to the statistical (1.2%) and systematic (2.2%) uncertainties summed in quadrature. It can be seen that the kinematical coverage includes both the quasielastic and delta-production peaks, and extends to the region in which the contribution of deep-inelastic scattering becomes appreciable. The statistical uncertainty includes beam charge (0.03%), detector and trigger efficiencies (0.1%), DAQ live-time (0.02%), VDC, and VDC track reconstruction efficiencies (0.1%) and uncertainties due to the charge-symmetric background prediction [40] (0.01%). A detailed list of the systematic uncertainties is given in Table I. All uncertainties are considered as fully uncorrelated. This new high precision C(e,e') data not only allowed us to carefully test our analysis framework and study systematics but also provides a vital information for the neutrino experiments that use carbon targets such as the long-baseline neutrino experiment T2K [41], NOvA [42] and neutrino interaction experiment MINERvA [43].

The solid line of Fig. 2 represents theoretical results obtained within the scheme described in Refs. [12, 14, 15, 44], based on the factorization *ansatz* dictated by the IA and the spectral function formalism. Note that this approach does not involve any adjustable parameters, and allows for a consistent inclusion of single-nucleon interactions—both elastic and inelastic—and meson-exchange current (MEC) contributions. The effects of FSI on the quasielastic cross section has been taken into account following the procedure developed in Ref. [44]. A detailed account of the calculation of the electron-carbon cross section will be provided in a forthcoming paper [45].

Figure 3 presents the inclusive electron-titanium cross section, measured at the same kinematics as for carbon and with an error up to ∼2.75%, sum in quadrature of statistical (1.65%) and systematic (2.2%) uncertainties. In the absence of any previous electron-scattering studies carried out using a titanium target, we determined the Ti(e,e') cross sections using:

$$\left(\frac{d^2\sigma^{\rm Born}}{d\Omega dE'}\right)^i_{\rm Ti} = \left(\frac{d^2\sigma^{\rm Born}}{d\Omega dE'}\right)^i_{\rm C} \times \frac{{\rm Yield}^i_{\rm Ti}}{{\rm Yield}^i_{\rm C}} \qquad (2)$$

where ${\rm Yield}^i_{\rm C/Ti}$ denotes the luminosity normalized yield respectively for C and Ti. By normalizing the yield ratio to published radiatively unfolded carbon cross sections $d\sigma_C^{\rm Born}$, we are implicitly unfolding bremsstrahlung from the quoted Ti cross sections. In this approach, most of the systematic uncertainties are fully correlated between C and Ti, due to the fact that the data was collected in the same kinematical setup and analyzed using the same cuts of the carbon data. Uncertainties due to radiative corrections, target thickness and density were evaluated independently for Ti, and added in quadrature to the uncertainties from C. Note that this is the first electron-titanium scattering data collected at the kinematics relevant for neutrino experiments. Therefore, the model of Refs. [12, 14, 15, 44], requiring as an input the target spectral function, could not be used to obtain theoretical results comparable to the data of Fig. 3.

Figure 4 shows the ratio

$$(d^2\sigma/d\Omega dE')/[Z\sigma_{ep}+(A-Z)\sigma_{en}]\ , \qquad (3)$$

for carbon and titanium,. Here σ_{ep} and σ_{en} denote the elastic electron-proton and electron-neutron cross sections stripped of the energy-conserving delta function. The difference between the results obtained using the measured carbon and titanium cross sections reflect different nuclear effects, that can be conveniently parametrized in terms of a nuclear Fermi momentum exploiting the concept of scaling of second kind, or superscaling [46]. The superscaling analysis of our data, illustrated in Fig. 5, suggests that the Fermi momentum in titanium is ∼240 MeV, to be compared to 220 MeV in carbon [47].

In this Letter, we have reported the first results of JLab experiment E12-14-012, consisting of the Ti(e,e') and C(e,e') cross sections at beam energy E = 2.222 GeV and scattering angle θ =15.541 deg. The quality

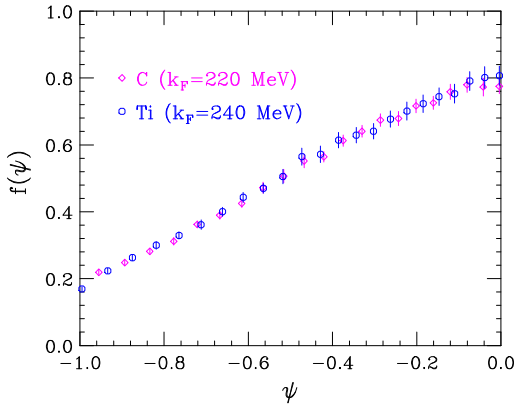

FIG. 5. (color online). Comparison between the scaling function of 2nd kind, $f(\psi)$, obtained from the E12-14-012 data on C and Ti, represented by diamonds and circles, respsctively. The Fermi momentum of carbon has been fixed to the value obtained by Moniz *et al.* [47]. The data analysis for Ti sets the Ti Fermi momentum at ∼240 MeV.

of the CEBAF electron beam and the excellent performances of the high resolution spectrometer and detector packages available in Hall A allowed for a quick and smooth data taking, and an accurate determination of the cross sections over the broad range of energy transfer in which quasielastic scattering—induced by both one- and two-nucleon currents—and resonance production are the main contributions to the inclusive cross sections.

Our titanium measurement, providing first electron-titanium scattering data at the kinematics relevant for neutrino experiments, will be of great value for the development of realistic models of the electroweak response of neutron-rich nuclei, which will be indispensable for the analysis of the next generation of neutrino oscillation studies employing argon detectors such as DUNE. Our carbon measurements provide a high precision data that can be utilized in the neutrino experiments that use carbon targets such as T2K, NOvA and MINERvA. Comparison between the results of theoretical calculations and carbon data confirms that the approach based on the spectral function formalism, supplemented by the inclusion of MEC and FSI contributions, provides a consistent framework, capable of providing a *parameter free* description of electron-nucleus scattering in the kinematical regime in which the IA is expected to be applicable.

We acknowledge the outstanding support from the Jefferson Lab Hall A technical staff, target group and Accelerator Division. The authors are indebted to N. Rocco for carrying out the calculation of the MEC contribution to the electron-carbon cross section shown in Fig. 2. This experiment was made possible by Virginia Tech and the National Science Foundation under CAREER grant No. PHY−1352106. This work was also supported by the DOE Office of Science, Office of Nuclear Physics, contract DE-AC05-06OR23177, under which Jefferson Science Associates, LLC operates JLab, DOE contracts DE-FG02-96ER40950 and DOE contracts DE-AC02-76SF00515.

[1] O. Benhar, P. Huber, C. Mariani and D. Meloni, Phys. Rept. **700**, 1 (2017).
[2] M. Antonello *et al.* (MicroBooNE, LAr1-ND, and ICARUS-WA104 Collaborations), arXiv:1503.01520 [physics.ins-det].
[3] R. Acciari *et al.* (DUNE Collaboration), arXiv:1512.06148 [physics.ins-det].
[4] K. Abe *et al.* (T2K Collaboration), Phys. Rev. D **88**, 032002 (2013).
[5] A. M. Ankowski *et al.*, Phys. Rev. D **92**, no. 7, 073014 (2015).
[6] M. Anghinolfi *et al.*, J. Phys. G**21**, L9 (1995).
[7] O. Benhar, *et al.* (The Jefferson Lab E12-14-012 Collaboration), arXiv:1406.4080 [nucl-ex].
[8] O. Benhar, Nucl. Phys. News **26**, 15 (2016).
[9] S. Frullani and J. Mougey, Adv. Nucl. Phys. **14**, 1 (1984).
[10] A. E. L. Dieperink and P. K. A. de Witt Huberts, Ann. Rev. Nucl. Part. Sci. **40**, 239 (1990).
[11] S. Boffi, C. Giusti, F. D. Pacati, Phys. Rept. **226**, 1 (1993).
[12] O. Benhar, N. Farina, H. Nakamura, M. Sakuda and R. Seki, Phys. Rev. D **72**, 053005 (2005).
[13] O. Benhar, D. Day, I. Sick, Rev. Mod. Phys. **80**, 189 (2008).
[14] A. M. Ankowski, O. Benhar, M. Sakuda, Phys. Rev. D **91**, 054616 (2015).
[15] N. Rocco, A. Lovato, O. Benhar, Phys. Rev. Lett. **116**, 192501 (2016).
[16] O. Benhar and D. Meloni, Nucl. Phys. A **789**, 379 (2007).
[17] O. Benhar, P. Coletti, and D. Meloni, Phys. Rev. Lett. **105**, 132301 (2010).
[18] O. Benhar and G. Veneziano, Phys. Lett. B **702**, 433 (2011).
[19] E. Vagnoni, O. Benhar, and D. Meloni, Phys. Rev. Lett. **118**, 142502 (2017).
[20] A. Lovato, S. Gandolfi, J. Carlson, S. C. Pieper and R. Schiavilla, Phys. Rev. Lett. **117**, 082501 (2016).
[21] A. Meucci and C. Giusti, Phys. Rev. D**89**, 117301 (2014).
[22] O. Lalakulich, U. Mosel and K. Gallmeister, Phys. Rev. C**86**, 054606 (2012).
[23] J. Nieves, F. Sanchez, I. Ruiz Simo and M. J. Vicente Vacas, Phys. Rev. D**85**, 113008 (2012).
[24] M. Martini, M. Ericson, G. Chanfray and J. Marteau, Phys. Rev. C**81**, 045502 (2010).
[25] V. Pandey, N. Jachowicz, T. Van Cuyck, J. Ryckebusch and M. Martini, Phys. Rev. C**92**, 024606 (2015).
[26] G. D. Megias, J. E. Amaro, M. B. Barbaro, J. A. Caballero, T. W. Donnelly and I. Ruiz Simo, Phys. Rev. D**94**, 093004 (2016).
[27] J. Heisenberg, J. S. Mccarthy and I. Sick, Nucl. Phys. A**164**, 353 (1971).

[28] A. M. Selig, C. De Vries, P. K. A. De Witt Huberts and I. E. Zacharov, Nucl. Phys. A**476**, 413 (1988).
[29] E. F. Romberg, N. S. Wall, D. Blum, J. W. Lightbody and S. Penner, Nucl. Phys. A**173**, 124 (1971).
[30] J. Alcorn *et al.*, Nucl. Instrum. Meth. A**522**, 294 (2004).
[31] J. Arrington *et al.*, Phys. Rev. Lett. **82**, 2056 (1999).
[32] Hall C Collaboration, paper in preparation
[33] MO. L. W. and TSAI, Y. S., Rev. Mod. Phys. **41**, 205 (1969).
[34] A. Aste, C. von Arx, and D. Trautmann, Eur. Phys. J. **A26**, 167 (2005).
[35] O. Benhar, D. B. Day, and I. Sick, arXiv:0603032 [nucl-ex]. http://faculty.virginia.edu/qes-archive/index.html
[36] I. Sick, D. B. Day, and J. S McCarthy, Phys. Rev. Lett. **45** , 871 (1980).
[37] J. S. O'Connell *et al.*, Phys. Rev. C **35**, 1063 (1987).
[38] R. M. Sealock *et al*, Phys. Rev. Lett. **62** (1989) 1350.
[39] D. B. Day *et al.*, Phys. Rev. C **48**, 1849 (1993).
[40] V. Tvaskis, PhD Thesis, Vrije Universiteit, Amsterdam, 2004.
[41] K. Abe *et al.* (T2K Collaboration), Nucl. Instrum. Meth, A659, 106 (2011).
[42] P. Adamson *et al.* (NOvA Collaboration), Phys. Rev. Lett. **118**, no. 23, 231801 (2017).
[43] L. Ren *et al.* (MINERvA Collaboration), Phys. Rev. D **95**, 072009 (2017).
[44] O. Benhar, A. Fabrocini, S. Fantoni, G. A. Miller, V. R. Pandharipande, and I. Sick, Phys. Rev. C **44**, 2328 (1991).
[45] O. Benhar and F. Coppini, paper in preparation.
[46] T.W. Donnelly and I. Sick,, Phys. Rev. C **60**, 065502 (1999).
[47] E.J. Moniz *et al*, Phys. Rev. Lett. **26**, 445 (1971).